ORIGINAL PAPER

Evaluation of canopy fraction-based vegetation indices, derived from multispectral UAV imagery, to map water status variability in a commercial vineyard

A. Berry[1] · M. A. Vivier[1] · C. Poblete-Echeverría[1]

Abstract

Water stress is a major factor affecting grapevine yield and quality. Standard methods for measuring water stress, such as midday stem water potential (Ψ_{SWP}), are laborious and time-consuming for intra-block variability mapping. In this study, we investigate water status variability within a 2.42-ha commercial Cabernet Sauvignon block with a standard vertical trellis system, using remote sensing (RS) tools, specifically canopy fraction-based vegetation indices (VIs) derived from multispectral unmanned aerial vehicle (UAV) imagery, as well as standard reference methods to evaluate soil and plant water status. A total of 31 target vines were monitored for Ψ_{SWP} during the whole growing season. The highest variability was at véraison when the highest atmospheric demand occurred. The Ψ_{SWP} variability present in the block was contrasted with soil water content (SWC) measurements, showing similar patterns. With spatial and temporal water stress variability confirmed for the block, the relationship between the Ψ_{SWP} measured in the field and fraction-based VIs obtained from multispectral UAV data was analysed. Four UAV flights were obtained, and five different VIs were evaluated per target vine across the vineyard. The VI correlation to Ψ_{SWP} was further evaluated by comparing VI obtained from canopy fraction (VI_{canopy}) versus the mean (VI_{mean}). It was found that using canopy fraction-based VIs did not significantly improve the correlation with Ψ_{SWP} ($NDVI_{canopy}$ $r = 0.57$ and $NDVI_{mean}$ $r = 0.53$), however fractional cover (f_{cover}) did seem to show a similar trend to plant water stress with decreasing canopy size corresponding with water stress classes. A subset of 14 target vines were further evaluated to evaluate if additional parameters (maximum temperature, relative humidity (RH), vapour pressure deficit, SWC and fractional cover) could serve as potential water stress indicators for future mapping. Results showed that the integration of $NDVI_{canopy}$ and $NDRE_{mean}$ with additional information could be used as an indicator for mapping water stress variability within a block.

Introduction

The study of spatial variability has received significant attention in the last two decades due to the fast-growing field of Remote Sensing (RS). The correct use of RS technologies could reduce the overall cost of agronomic management (Cinat et al. 2019). In viticulture, the use of proximal and RS tools for monitoring vineyards has become increasingly popular and offers a non-destructive and efficient way of collecting data, which can provide valuable insight into the variability in and among vineyards. With-in vineyard, or intra-block variability is not a new concept, and RS has already proven its potential in spatio-temporal evaluation (Khaliq et al. 2019), however the accuracy of mapping true vineyard variability for the purpose of precision viticulture (PV) still remains a challenge, particularly due to components (soil, shadows, cover corps) interfering with the calculation of vegetation indices (VIs). RS data enable the characterization of plant physiology through the computation of VIs, such as the widely recognized normalize vegetation index (NDVI). NDVI takes advantage of the distinct reaction of vegetation to the visible (red) and near-infrared bands, closely linked to the conditions of crops (Matese and Di Gennaro 2015). Unmanned aerial vehicle (UAV) imagery has been widely utilized in various agricultural applications, specifically were VIs have been used for assessing plant vigour, biomass production, disease detection, nitrogen content

✉ C. Poblete-Echeverría
cpe@sun.ac.za

1   South African Grape and Wine Research Institute
    (SAGWRI), Faculty of AgriSciences, Stellenbosch
    University, Matieland 7602, South Africa

analysis and crop water stress evaluation. The disadvantages of UAVs however, include their dependence on the sensing technologies they carry for data acquisition, the need for flying permits and compliance with regulations, and limitations in operation during adverse weather conditions (Tardaguila et al. 2021; Poblete-Echeverría and Tardaguila 2023; Gautam and Pagay 2020).

Most recent studies place focus on how to incorporate machine learning or classification algorithms in these approaches (Filippetti et al. 2013; Gatti et al. 2017; Di Gennaro et al. 2018; Romboli et al. 2017; Cinat et al. 2019; Karpina et al. 2016; Matese et al. 2019; Kerkech et al. 2020). The effectiveness of VIs has been explored across different RS platforms, including aircraft, satellite-based and UAV observations (Matese et al. 2015; Tardaguila et al. 2021). However, UAVs have emerged as a popular RS tool due to their ability to acquire images at low altitudes with high spatial resolution (Pádua et al. 2018; Cinat et al. 2019). UAVs are considered the most advanced platform for RS, and their application continue to progress with advancement in technology (Matese et al. 2018). Moreover, UAVs offer advantages such as low manufacturing costs and greater flexibility in acquiring frequent temporal data, overcoming some limitations associated with satellite-based observations. In a recent review article published by Giovos et al. (2021), 113 publications reviewed made use of RS to calculate VIs, specifically NDVI, for one of three applications, monitoring, estimating vine water stress or delineation of management zones (Caruso et al. 2017; Di Gennaro et al. 2019; Khaliq et al. 2019; Sozzi et al. 2020; Giovos et al. 2021).

Grape berries under mild or moderate water deficit during the ripening period, is known to concentrate sugars and some phenolics, whereas severe water stress can adversely affect the quality of berries reducing sugar and aroma levels, as well as lowering grape yields (e.g., van Leeuwen et al. 2009, 2018). Therefore, precision irrigation techniques that consider the spatial variability of soil and plant characteristics will help farmers avoid overwatering or underwatering their vineyards at the key developmental stages. Additionally with the agriculture sector consuming 70% of the worlds water resources with intensity and frequency of droughts still on the rise, the need for precision irrigation techniques is becoming more crucial (Gilbert 2012; Stocker et al. 2013; Gago et al. 2015). Monitoring water status in future will therefore become necessary during grapevine developmental stages to ensure grape quality and sustainability when accessible irrigation water is limited (Espinoza et al. 2017; Rodríguez-Pérez et al. 2018; Zúñiga et al. 2018; Ezenne et al. 2019). While emphasizing the importance of monitoring and mapping spatial variability associated with water stress response in grapevines, it is also essential to consider extending these efforts to capture the seasonal dynamics. Ideally, the goal is to comprehensively map spatial variability over time scales, including the seasonal variation. By incorporating the temporal aspect into the analysis, we can not only develop effective vineyard management practices, but also optimize yield and quality for sustainable production.

In context of grapevine water stress assessment, understanding the physiological responses of grapevine to mild or moderate water stress is crucial for optimizing deficit irrigation timing and amount (Chaves et al. 2007, 2010). Biophysical restrictions, such as inadequate soil water availability, are likely to cause grapevine canopies to reflect less light, resulting in smaller NDVI values compared to larger, healthier, and well water canopies (Baluja et al. 2012; Gautam and Pagay 2020). However, unlike individual vine detection which enables the estimation of biophysical and geometrical parameters, the calculation of NDVI involves averaging the values across the entire area of interest without focusing solely on the canopy fraction (Pádua et al. 2020). Previous studies have demonstrated the successful application of UAV-based RS for soil moisture monitoring, water consumption, use efficiency, and surface energy budget analysis in grapevines (Hassan-Esfahani et al. 2015; Thorp et al. 2018; Gago et al. 2015). A study conducted by Tang et al. in 2022, which focused on leaf water potential, demonstrated great potential. They developed a unified machine learning model using multispectral RS imagery and weather data, which was able to capture patterns both within and across fields by using Random Forest analysis capturing 77% of the variance. These are just a few examples highlighting the potential of UAV-based RS in improving vineyard management for water resource utilization.

However, accurately identifying and delineating various components of vineyards, such as canopy, soil, shadows, and cover crops, remains one of the most actively studied challenges in literature as these components may introduce interferences and lead to biased crop status assessments when calculating VIs. When satellite or aircraft-based observation are made, RS indices are affected by these mixed pixels (components) mainly due to lack of resolution (Suárez et al. 2008; Rossini et al. 2013; Santesteban et al. 2017; Zarco-Tejada et al. 2013). This challenge, as explained by Dobrowski et al. (2002), is due to the discontinues nature of vine rows, their moderate coverage, soil influences, background and shade that pose a challenge to RS analysis and therefore suggested that pixels should be separated. Although this problem (mixed pixels) mainly persists in low-resolution data, that cannot be separated, for example satellite-based images, high-resolution UAV data allow for easier classification of these conditions. Once these elements are classified (for example pure grapevine vegetation) they can be used to apply other classification approaches in their pixels (Burgos et al. 2015). To overcome these challenges of pure vs mixed pixel, researchers have actively explored new

methodologies that aim to address these limitations with photogrammetric processing techniques for detecting inter-row spaces or missing plants (de Castro et al. 2018; Cinat et al. 2019; Pádua et al. 2020). Kerkech et al. (2020) looked at optimized image registration and deep learning segmentation approaches as an application for disease detection in grapevine. Maimaitiyiming et al. (2020) proposed canopy zone-weighting (CZW) methods in estimating physiological indicators making use of neural net classifier Canny edge detection to extract pure vine canopy data. In more recent studies a strong focus was placed on developing new automated methodologies to achieve precise representation of vineyard components, particularly using machine learning algorithms and classification methods to automate the process and minimize human involvement. These innovative approaches include the utilization of (artificial neuron network) ANN models, (Hue, saturation, and value) HSV-based algorithms, (digital elevation model) DEM models, K-means unsupervised algorithms, techniques, additionally, combinations of these techniques have also been explored (Huang et al. 2011; Calvario et al. 2017; de Castro et al. 2018; Cinat et al. 2019; Pádua et al. 2022).

Despite numerous efforts by researchers to address the complications arising from mixed pixels there continues to be ongoing exploration for more streamlined and precise approaches. In recent years, the concept of fractional cover (f_{cover}) has emerged as a potential solution to this limitation. f_{cover} refers to the proportion of the land surface covered by a given vegetation type, in this case grapevine canopy (Liu et al. 2012). The f_{cover} can be estimated using various RS techniques as previously mentioned (ANN-models, HSV-based algorithms, DEM models and K-means), but these studies however did not focus on individual vines but on inter-block or regional scale by evaluating seasonal models for prediction purposes. It is important to note that monitoring and evaluating vines throughout the season could improve the application of crucial corrective management actions to limit or manage variations effectively. f_{cover} enables the quantification of the vegetation in a particular area, which informs on growth and development by monitoring the plant responses to environmental stressors, such as water deficit. The assumption is that by providing information on the spatial distribution and density of vegetation, linked to water stress, informed decisions about irrigation strategies and management practice could ensure optimal vine health and grape production.

In the pursuit of advancing vineyard management techniques, this study takes a distinctive approach by utilizing RS tools typically used for larger-scale mapping and applying them to intra-block mapping. In this study, the objective was to apply and test fraction-based segmentation analysis to achieve pure canopy VI of $n = 31$ individual target vines in a commercial vineyard. Field data measurements of Ψ_{SWP} and

soil water content (SWC) were correlated to pure (VI_{canopy}) and mixed pixel (VI_{mean}) data and compared to evaluate if exclusion of soil and other objects through pure canopy extraction could improve the use of VIs as water stress indicators for the monitoring of intra-block variability over a typical season. Additional micrometeorological data (maximum temperature, relative humidity (RH), vapour pressure deficit) were collected on a subset of the target vines ($n = 14$) to evaluate their potential to serve as water status indicators for variability mapping.

Materials and methods

Site description

During the 2019–2021 growing seasons, a field experiment was implemented on Thelema Mountain vineyards, a commercial farm situated in the Stellenbosch wine region of South Africa at coordinates 33°54′11.8″S—18°55′12.4″E and an elevation of 430 m above sea-level. The selected block was a 2.42 ha Cabernet Sauvignon vineyard planted in 2003 on a standard vertical shoot positioning (VSP) trellis system with a North/South row direction. The vine spacing was 2 m and the inter-row width was 2.5 m. The first season of monitoring in this vineyard is fully described in Jasse et al. (2021). Based on the seasonal Ψ_{SWP} data from the 2019/2020 season (reported in Jasse et al. 2021), water stress was observed, and the block was mapped according to three water stress classes (Fig. 1). In the second season (2020/2021; this study) $n = 31$ target vines were selected within these three water stress classes for further data collection. The target vines were monitored on a weekly basis for Ψ_{SWP} and SWC. This data served as ground truthing, using reference methods, to allow comparison with RS data collected for the site.

Field measurements

Stem water potential

Midday stem water potential (Ψ_{SWP}) was used as the reference method to define the water status of the vines. Measurements were taken weekly around midday (12:00 to 13:00 local time), from November to March by means of a pressure chamber (PMS Instrument Company, model 1505D, Albany, USA). Healthy leaves from the middle of the canopy, facing the shaded side were selected. To limit leaf transpiration each selected leaf was covered with aluminium foil inside a plastic zip bag at least 1 h before midday measurements (Choné et al. 2001).
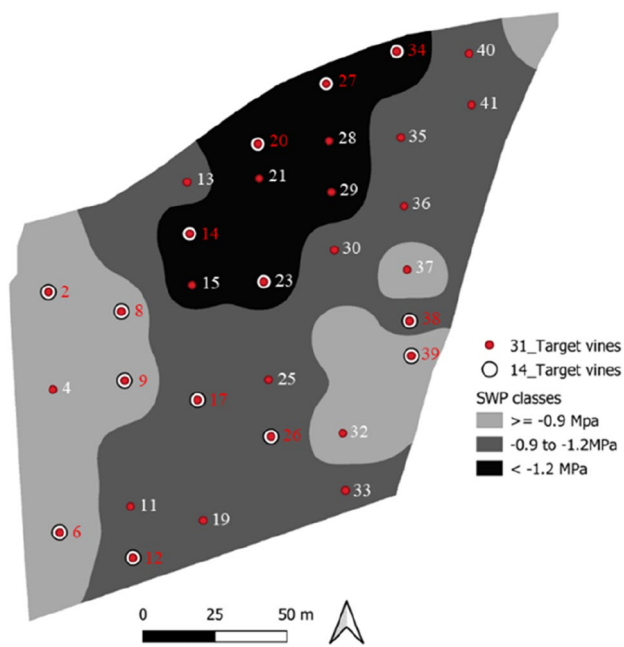
Fig. 1 The spatial map is coloured according to three water stress classes (Class 1 > −0.9 MPa; Class 2 between −0.9 and −1.2 MPa and Class 3 < −1.2 MPa), based on midday stem water potential (SWP) as reported in Jasse et al. (2021). Red numbered dots on the map indicate the locations of $n = 31$ target vines, where reference measurements were conducted during the 2020–2021 season. Additionally, micrometeorological data were collected for $n = 14$ of the target vines, spanning all three water classes; these vines are indicated by white circle around the numbered red dots

Soil water content

In-soil monitoring was done by using a Neutron probe. Relative SWC measurements were obtained from November to March, at 20 and 40 cm depth (root zone) using a Neutron Probe (CPN International, model 503DR Hydroprobe, CA, USA). Measurements were taken for all target vines (Fig. 1). PVC plastic pipes with 50 mm diameter and endcaps, were inserted at a depth of 50 cm at the target vines. The permanent wilting point (PWP) and field capacity (FC) was determined using Soil Plant Atmosphere Water (SPAW) software developed by Saxton et al. (2006).

Temperature and relative humidity

Daily meteorological data for the block were measured hourly by a standard commercial weather station located within 300 m of the field experiment. Additionally, temperature (Temp) and RH variables were measured during the season using Tinytag® loggers (TinyTag Plus 2—TGP4500, Gemini Data Loggers (UK) Ltd., Chichester, United Kingdom). Sensors were installed in the bunch zone of 14 target vines (Fig. 1). These loggers were installed form November

2020 to March 2021, logging every 15 min. Maximum temperature and corresponding RH was mapped to give context to water stress in this study. Vapour pressure deficit (VPD) was calculated for each target vine, using the available microclimate data to explore the atmospheric demand for water.

Remote sensing

Unmanned aerial vehicle (UAV) flights

Visible–near infrared (VIS–NIR) spectral information acquired with UAV was obtained from a commercial company (Caelumn Technologies, South Africa). The UAV was equipped with a Phantom 4 Pro with MicaSense RedEdge TM₃ Multispectral camera (MicaSence Inc., Seattle, WA, USA), 20Mp HD camera. The multispectral bands included in order blue (460–510 nm), green (545–575 nm), red (630–690 nm), near infrared (820–860 nm), and red edge (712–722 nm) to capture different analytical layers. Ground checkpoints served as reference points to georeferenced each individual vine within the World Geodetic System (WGS). For enhanced precision, Caelumn Technologies incorporated ground control points. UAV image capture was scheduled between 11 am and 2 pm, closely aligned with solar noon, to minimize the influence of shadows. Consistency was maintained by employing the same flight plan across all drone flights. Images were taken at 60 m with a resultant pixel size of 5 cm resolution. The drone image was calibrated using a reflectance image obtained on the flight day and multispectral images were mosaicked and geo-corrected using Agisoft PhotoScan® Software (version 1.2.5 Agisoft LLC, St Petersburg, Russia). UAV flights were captured four times during the season. Figure 2 depicts a summary of measurements taken during the growing season, with a main focus on four developmental stages, to evaluate the suitability of VI to accurately map the water status variability present in the block. Winter pruning occurred in August, while the remainder of the block was uniformly managed with two top actions at the beginning of the year.

UAV vine segmentation

The method used for vineyard segmentation and individual target vine identification is shown in Fig. 3. The steps include image acquisition, mosaicking and geo-correction as explained in section "Unmanned aerial vehicle (UAV) flights". QGIS (QGIS 3.16.8, Hannover) software was used to manually isolate the georeferenced target vines from RGB and multispectral images. The segmentation and classification of images, a crucial step in the image analysis process, were carried out with specific attention to detail. To achieve this, a systematic approach was employed using the QGIS

DOY	307	314	321	342	363	04	11	18	25	32	39	46	53	60
E-L stage*					E-L33		E-L34		E-L35				E-L38	
Ψ_{SWP}	✓	✓	✓	✓	✅	✓	✅	✓	✅	✓	✓	✓	✅	✓
SWC	✓	✓	✓	✓	✅	✓	✅		✅	✓		✓	✅	✓
UAV					🛸		🛸		🛸				🛸	
f_{cover}					✅		✅		✅				✅	
Temp**					✅		✅		✅				✅	
RH**					✅		✅		✅				✅	
VPD**					✅		✅		✅				✅	

Fig. 2 Provides a summary of measurements taken from November 2020 to March 2021, represented by days of the year (DOY). The measurements include midday Ψ_{SWP} and soil water content (SWC), which were regularly recorded and indicated by black tick marks. At four developmental stages (E-L33, E-L34, E-L35 (véraison), E-L38 (harvest)), all parameters including Ψ_{SWP}, SWC and UAV flights were conducted, with resulting f_{cover} data for $n=31$ target vines. Additionally, maximum Temperature (Temp) and relative humidity (RH) as well as vapour pressure deficit (VPD) was available for these days for $n=14$ target vines. *E–L stage: Eichhorn–Lorenz scoring system (Eichhorn and Lorenz 1977; Coombe 1995). **Values available for $n=14$ target vines

software. First, a project file named "QGIS Drone cutting" was established. Within this project, a 2.5 m × 2 m polygon was created using the rectangle function with precise measurements. This polygon served as a template to ensure accuracy and consistency. It was then georeferenced and adjusted to match the location of each target vine, effectively creating a tailored cutting template. Using this template, vector clipping was performed, enabling the isolation of individual target vines from the larger dataset. Importantly, this process was executed for both the multispectral and RGB drone images. The RGB-polygon was converted into a black and white mask using MATLAB colour thresholding app to isolate only the canopy fraction (f_{cover}). Calculated VIs are listed in Table 1. The chosen VIs (NDVI, NDRE, GNDVI, NGRDI, and SAVI) were selected based on previous research indicating their potential sensitivity to water stress and their demonstrated ability to detect changes in plant health and water content (Ahmad et al. 2021; Cogato et al. 2022; Espinoza et al. 2017; Pagay and Kidman 2019; Tang et al. 2022; Tiozzo Fasiolo et al. 2023). Values calculated for the whole polygon area (VI_{mean}) correspond to an average of all pixels represented in the polygon (2.5 m × 2 m). The canopy area (VI_{canopy}) considered only the canopy fraction consisting of pure pixels. The f_{cover} mask was overlayed with multispectral image to isolate the pure canopy pixels.

Statistical analysis

To get a basic overview of the variability present in the 2020–2021 season, R software (R v4.1.2; R Core Team, 2019) was used to analyse the weekly Ψ_{SWP} in the form of boxplots. Basic descriptive analysis was done to calculate average, minimum and maximum as well as % coefficient of variation (%CV). Next the Ψ_{SWP} dates that correlated with UAV flights were visually mapped using QGIS (QGIS 3.16.8, Hannover) to evaluate spatial water stress patterns. The same was done to evaluate SWC patterns.

Multivariate data analysis was used to explore RS data comparing VI_{mean} and VI_{canopy} using principal component analysis (PCA) plots in SIMCA (SIMCA version 16.0.2 from MKS Data Analytics and Solutions). Furthermore, relationships between field Ψ_{SWP} measurements and VI_{canopy}
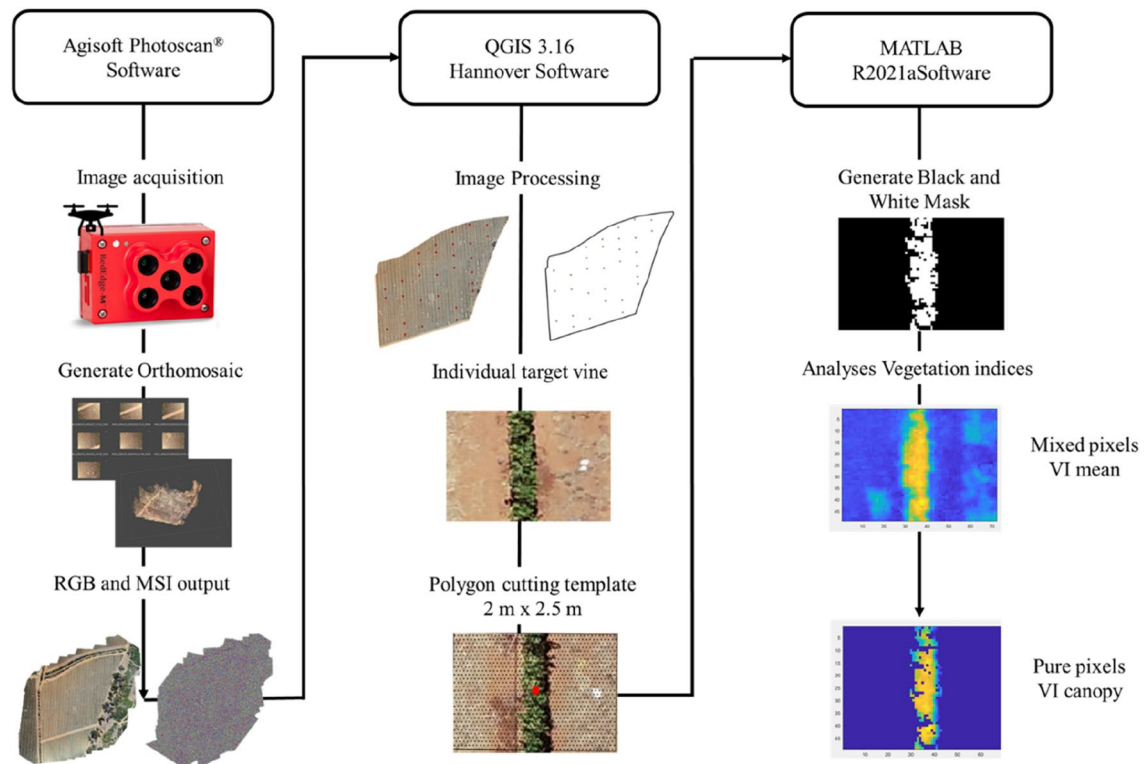
Fig. 3 Image acquisition and segmentation of individual target vines are presented as follow: image acquisition was done with a MicaScence RedEdge multispectral camera. The RGB and MSI output was further processed using QGIS software to identify the individual target vines using georeferenced location and additional white rock markers. A 2.5 m × 2 m polygon was used to cut the individual target vines form the RGB and MSI. The RGB polygon was first converted to a black and white mask in MATLAB to isolate f_{cover}. The entire polygon was used to calculate the VI_{mean} (mixed pixel), whereas the black and white mask was used to only calculate the VI_{canopy} (pure pixel) of the f_{cover}

Table 1 Vegetation indices (VIs) used in this study to calculate either VI_{canopy} or VI_{mean}

Abbreviation	Vegetation index (VI)	Equation	References
NDVI	Normalized difference vegetation index	$NDVI = \frac{NIR-Red}{NIR+Red}$	Rouse et al. (1974)
GNDVI	Green normalized difference vegetation index	$GNDVI = \frac{NIR-Green}{NIR+Green}$	Gitelson and Merzlyak (1997)
NDRE	Normalized difference red edge index	$NDRE = \frac{NIR-rededge}{NIR+rededge}$	Barnes et al. (2000)
NGRDI	Normalized green–red difference index	$NGRDI = \frac{Green-red}{Green+red}$	Motohka et al. (2010)
SAVI	Soil adjusted vegetation index	$SAVI = 1.4 \times \frac{NIR-red}{NIR+red+0.4}$	Huete (1988)

and VI_{mean} was explored by Pearson correlation coefficients (r) for individual dates ($n = 31$) as well as combined for the season ($n = 124$). f_{cover} was further explored by spatial maps (QGIS) to compare the Ψ_{SWP} and SWC maps.

Additional ($n = 14$) field data for maximum temperature, RH and VPD were first explored by spatial maps (QGIS). Lastly to evaluate the potential of combined water stress indicators, the $n = 14$ meteorological data were combined with SWC for 20 and 40 cm, f_{cover}, $NDVI_{mean}$, $NDRE_{mean}$, $NDVI_{canopy}$, and $NDRE_{canopy}$ for all four dates ($n = 56$). A pairwise scatterplot matrix was constructed using the *ggcorrplot* packaging in R software. All statistical tests were conducted at the level of significance, and all reported *p*-values are two-tailed.

Results

Overview of the intra-block variability in water status

Ψ_{SWP} measurements done during the season (2020–2021) are summarized in Fig. 4. The boxplots (Fig. 4a) indicated an increase in Ψ_{SWP} variability during the season. The CV for Ψ_{SWP} measurements across the season ranged from 10.18% to 26.25%. The maximum variability was present during the véraison period (DOY 18, 25, 32) with DOY 25 having the highest CV 26.25%. Outliers present in DOY 39 and 60 were noted as P13 and P14 which were represented in the previous season by the water stress Class 2 and 3, with P14 being the most stressed target vines throughout. The boxplot (Fig. 4b) shows the average variation in Ψ_{SWP} across the months for November (CV 15.68%), December (CV 23.10%), January (23.16%) and February (CV 23.70%) increasing towards harvest.

Spatial variability maps for Ψ_{SWP} and SWC (20 and 40 cm) on the days corresponding to UAV drone flights (DOY: 363, 11, 25, 53) are presented in Fig. 5. Ψ_{SWP} maps are coloured according to the thresholds of the three water stress classes (class 1 > −0.9 MPa, class 2 between −0.9 and −1.2 MPa and class 3 < −1.2 MPa) with added descriptive analysis data for average, %CV, minimum and maximum values for each day. Spatial map for DOY 363 shows although variability was present (CV 23.4%) all target vines Ψ_{SWP} levels were > −0.9 MPa (blue) with no water stress present in the block at that stage. First signs of medium stress (yellow) are present at DOY 11 at the top area of the block having values representative of Class 2. At DOY 25, all three water classes (blue, yellow, red) are present in the block with stress increasing from the bottom to the top part of the block. At DOY 53, severe stress (Class 3) was prominent in the top part of the block showing the same trend of stress that was present in the previous season. SWC values are presented in Fig. 5 for two depths (20 and 40 cm) and are coloured according to five levels. PWP and FC is noted in the figure for each depth as well as irrigation and rain events. The 20 cm depth ranged between 30 and 90 mm with irrigation and rain events contributing to an increase in water measured. All points were above the PWP, although the top of the block indicated dryer areas (30–60 mm) toward the end of the season corresponding with Ψ_{SWP} maps. The 40 cm depth ranged between 90 and 150 mm with the deeper soil drying out towards the end of the season without any point reaching below PWP although some plants experienced high stress according to class 3 represented at the top of the block (Ψ_{SWP}). Throughout the season it is notable that the top part of the block has lower SWC that the bottom; this was visible in both the 20 and 40 cm depths. We also see the impact of irrigation as the season progressed. The differences in the three classes are small yet the corresponding Ψ_{SWP} for the last two dates are more pronounced, confirming the SWC alone cannot give you a good view of water stress.

Remote sensing

Exploring vegetation indices

The five VIs (NDVI, GNDVI, NGRDI, NDRE and SAVI) used in this study were obtained using a mean approach (i.e. an average of the whole area assigned for the vine) and a selective approach (i.e. pure canopy, excluding the soil pixels). Table 2 summarizes the average VI values for VI_{mean} and VI_{canopy} during the season. Overall, very
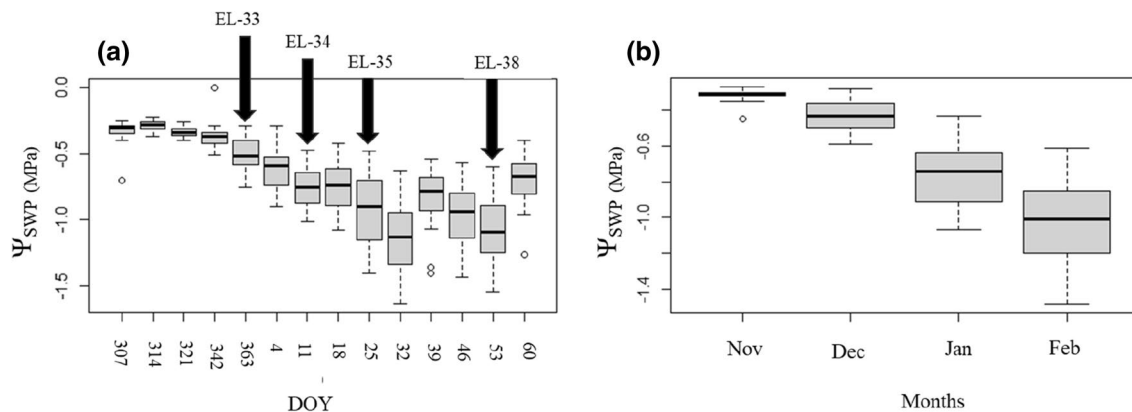
Fig. 4 Ψ_{SWP} measurements taken from November 2020 (DOY 307) to March 2021 (DOY 60). **a** Intra-block variability visible during the season becoming more severe towards the end of the season. This is indicated by the whiskers in the boxplot increasing in length showing an increase in the range of values. **b** Average monthly Ψ_{SWP} present in the block for November, December, January, and February. Circles represent extreme outliers which are linked to Plant 13 and 14. Black arrows indicate the four EL-stages when UAV flights were conducted
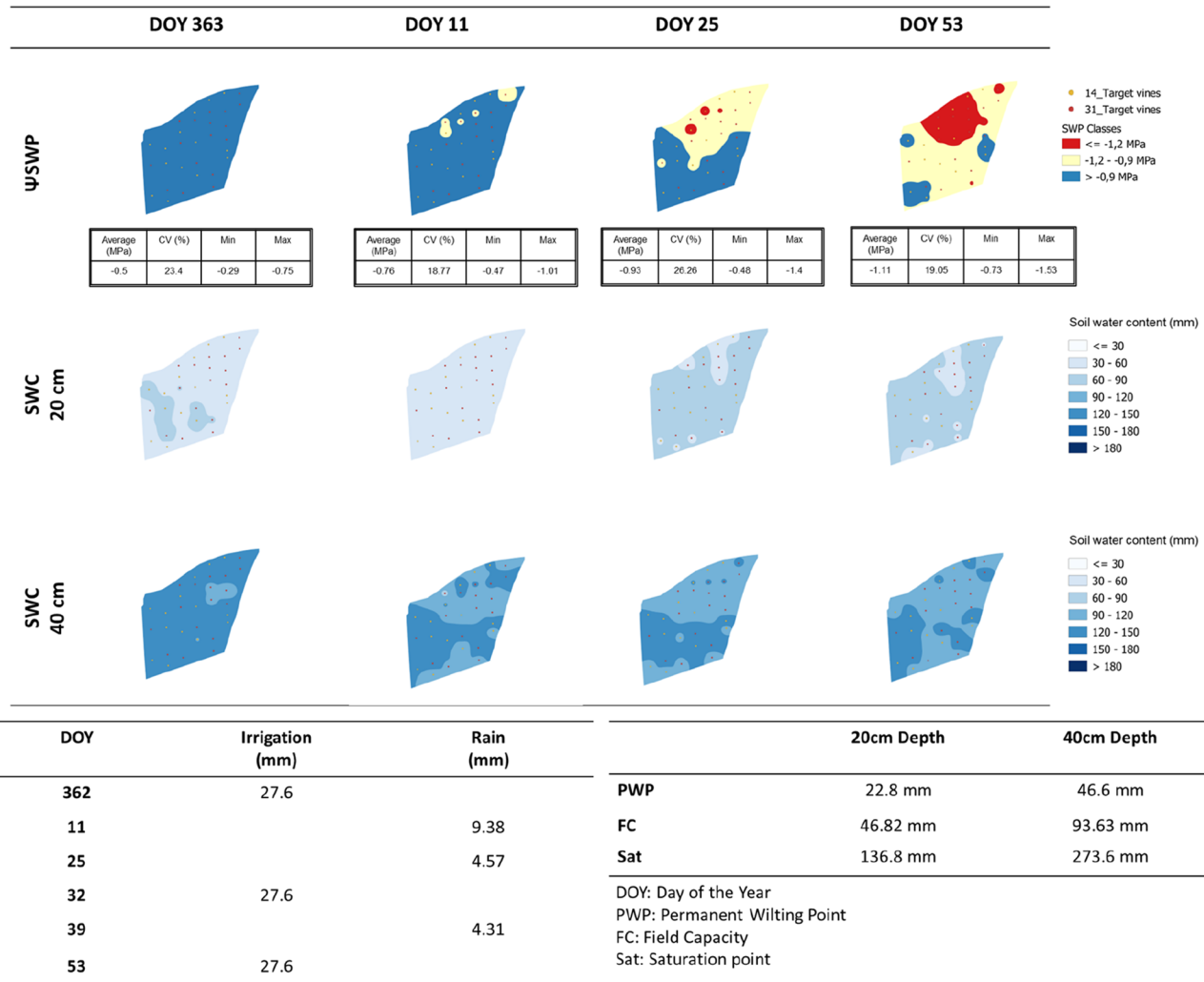
Fig. 5 The figure illustrates the spatial distribution of Ψ_{SWP} patterns across the block, along with corresponding SWC information for four specific DOY. The maps depict Ψ_{SWP} coloured according to three water stress classes. Additionally, SWC data are presented for two depths (20 and 40 cm). The figure includes reference points such as permanent wilting point (PWP), field capacity (FC) and saturation point. Days of irrigation and rainfall events are indicated according to DOY

Table 2 Display average calculated VIs for VI_{mean} and VI_{canopy} for four dates

Vegetation index	DOY 363		DOY 11		DOY 25		DOY 53	
	Mean	Canopy	Mean	Canopy	Mean	Canopy	Mean	Canopy
NDVI	0.060	0.394	0.041	0.361	0.009	0.281	−0.003	0.279
GNDVI	0.031	0.110	−0.010	0.074	−0.007	0.076	−0.025	0.077
NGRDI	0.032	0.269	0.075	0.255	0.017	0.189	0.023	0.189
NDRE	0.035	−0.086	0.002	−0.117	0.013	−0.168	0.059	−0.121
SAVI	0.063	0.290	0.031	0.236	−0.012	0.194	−0.012	0.194

$n = 31$ target vines for each date

low values were obtained for VI_{mean} compared to VI_{canopy}, which was expected due to a large portion being bare soil. NDVI values present normal to moderate vegetation during DOY 363 for early stages when grapevine is still actively growing. Thereafter, an overall decline is seen toward harvest indicating maturation or senescence as the season progressed.

The data were evaluated with multivariate data analysis by performing a PCA (Fig. 6). For both VI_{canopy} and VI_{mean} separation was observed between the phenological stages
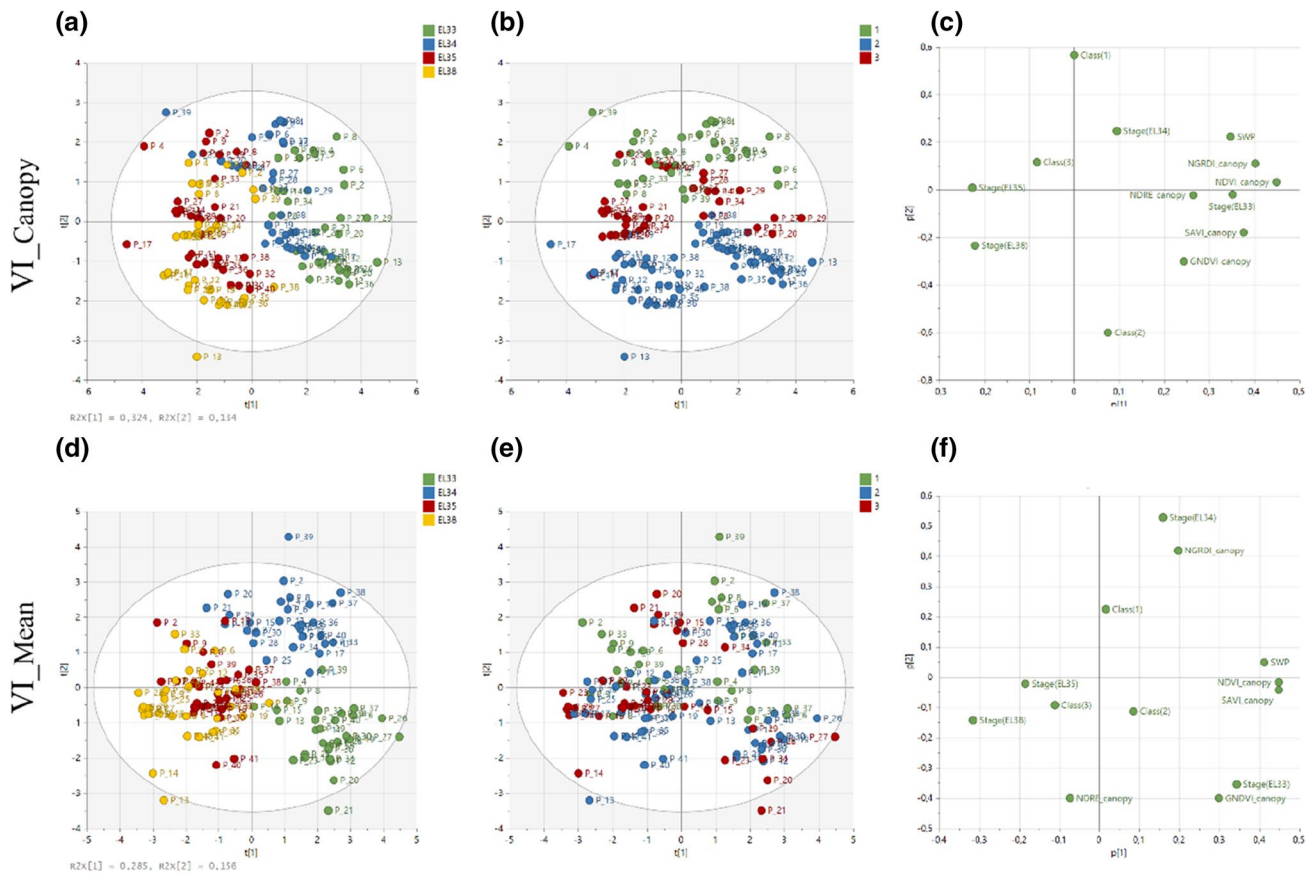
Fig. 6 Multivariate data analysis used to perform principal component analysis on the VI$_{mean}$ and VI$_{canopy}$ data. PCA for VI$_{canopy}$ (**a**) and VI$_{mean}$ (**d**) coloured according to four developmental stages for DOY 363 (E-L33), DOY 11 (E-L34), DOY 25 (E-L35), DOY 53 (E-L38).

PCA for VI$_{canopy}$ (**b**) and VI$_{mean}$ (**e**) coloured according to water stress classes 1, 2 and 3 with corresponding loadings plot for VI$_{canopy}$ (**c**) and VI$_{mean}$ (**f**)

as well as water stress classes. VI$_{canopy}$ showed slightly better separation for component 1 with 32.4% (Fig. 6a) of the variance explained compared to VI$_{mean}$ 28.5% (Fig. 6d). Although VI$_{mean}$ seemed to have better groupings for phenological stage, VI$_{canopy}$ could clearly be grouped according to water stress classes (1, 2 and 3). This could be due to values for VI$_{canopy}$ being similar (per class) due to the excluding of mixed pixels mostly represented by the soil area. In both VI grouped in the early stages (E-L33, E-L34) more towards NDVI and GNDVI driving the separation in the first and second quadrant visible in the loading's plots (Fig. 6c, f) linking to active growth and lower water stress levels. Also visible in Fig. 6 are the two extreme plants (P13, P14) that experienced highest water stress according to the reference methods (E-L38).

To further explore the relationship between VIs and water stress, a Pearson correlation analysis was performed (Table 3). The analysis evaluated the correlation between each of the five VIs obtained from VI$_{mean}$ and the VI$_{canopy}$ with Ψ_{SWP}, SWC and fractional cover (f_{cover}) as a measure

of water stress for separate dates ($n = 31$) as well as all dates combined ($n = 124$). The results of the analysis provide insight into the strength of the relationships between the different VIs and Ψ_{SWP}. In general data showed better correlation between VI$_{mean}$ with Ψ_{SWP} compared to VI$_{canopy}$. The best correlations were found on DOY 53, when all water stress classes were present. Considering the VI$_{mean}$, which incorporates information from the surrounding areas such as the soil, could potentially exhibit a better correlation with Ψ_{SWP}. When all data points are grouped, the correlation increase for NDVI$_{mean}$ $r = 0.53$ and NDVI$_{canopy}$ $r = 0.57$, respectively. Visual representation of NDVI$_{mean}$ and NDVI$_{canopy}$ can be seen in Fig. 7. Here we observed that the spatial map for VI$_{mean}$ exhibited a better correspondence with Ψ_{SWP} maps, although the agreement was not exceptionally strong. Notably, this correspondence became clearer towards the end of the growing season when clear distinctions between the water stress classes were present. VI$_{canopy}$ did not show good corresponding maps.

Table 3 Display Pearson correlations between calculated VIs for VI_{mean} and VI_{canopy} and midday stem water potential (Ψ_{SWP}), SWC and fractional cover (f_{cover}) measurements for individual dates ($n=31$) as well is for the seasonal combined data set ($n=124$)

Vegetation index	DOY 363 $n=31$		DOY 11 $n=31$		DOY 25 $n=31$		DOY 53 $n=31$		All $n=124$	
	Mean	Canopy	Mean	Canopy	Mean	Canopy	Mean	Canopy	Mean	Canopy
NDVI	−0.04	−0.15	0.31**	0.05	−0.25	0.02	0.62***	0.35**	0.53***	0.57***
GNDVI	−0.09	−0.13	0.36	0.32	−0.34*	0.00	−0.07	−0.17	0.30***	0.24***
NGRDI	0.06	−0.10	−0.11	−0.25	0.19	0.17	0.64***	0.28	0.19**	0.47***
NDRE	−0.35**	−0.17	−0.18	−0.30	−0.23	−0.48***	0.22	0.03	−0.13	0.14
SAVI	−0.08	−0.13	0.20**	−0.06	−0.39**	0.14	−0.36**	0.07	0.22**	−0.22**

Significance levels are indicated by * $p < 0.1$, ** $p \leq 0.05$ and *** $p \leq 0.01$

Fig. 7 The figure illustrates the spatial distribution of NDVI for both mean and canopy patterns across the block, for four specific DOY

The role of fractional cover

While VI_{canopy} did not show the best potential in the monitoring of water stress, VI_{mean} does not provide a complete picture of the water stress conditions of the vines. One limitation is that VI_{mean} measures are based on average of spectral signatures, whereas VI_{canopy} provides context on fractional cover (f_{cover}) by segmenting the canopy. In this section, we mapped (Fig. 8) the f_{cover} obtained from the UAV imagery to characterise the water stress in the vineyard. The spatial maps revealed interesting patterns in the distribution of vegetation across the study area. In the early stages (Fig. 8a) of the growing season, the f_{cover} appeared to correspond with areas of the bottom of the block that in general had higher SWC, showing bigger f_{cover} values. As the season progressed, the f_{cover} became more stable across the block (Fig. 8b) except for the (class 3) water stress area showing smaller f_{cover} at the top of the block also corresponding to the area that had lower SWC. The spatial maps suggest that f_{cover} appear to be driven by variations in plant stress levels, with areas of higher stress showing lower f_{cover}. This suggests that f_{cover} can serve as a

potential indicator of plant stress. It is however important to note that the response of the canopy to water stress is not immediate and that it takes time for changes in water availability to reflect in the vegetation cover. Therefore, monitoring changes in f_{cover} over time by using spatial maps can provide a good indication of water stress levels on an intra-block level.

To show the relationship between f_{cover} and Ψ_{SWP}, three target vines (P2, P26, P14), representing water stress class 1, 2 and 3, respectively, were compared for f_{cover} and the corresponding Ψ_{SWP} value (Fig. 9). Class 1 ($>−0.9$ MPa) with low water stress, had an initial increase in f_{cover} which stabilized towards harvest. The same can be seen for the corresponding Ψ_{SWP}, with increase in canopy size the Ψ_{SWP} values increase stabilizing toward harvest never not changing water stress class. Class 2 ($−0.9$ to $−1.2$ MPa) showed increase in f_{cover} during the season with a more prominent reduction in f_{cover} towards harvest. Ψ_{SWP} values gradually increased during the season. Class 3 ($<−1.2$ MPa) showed a definite decrease in f_{cover} with noticeable increase of Ψ_{SWP} throughout.

(a)

(b)

(c)

(d)

14_Target vines
31_Target vines

fcover (%)
<= 6,0
6,0 - 12,0
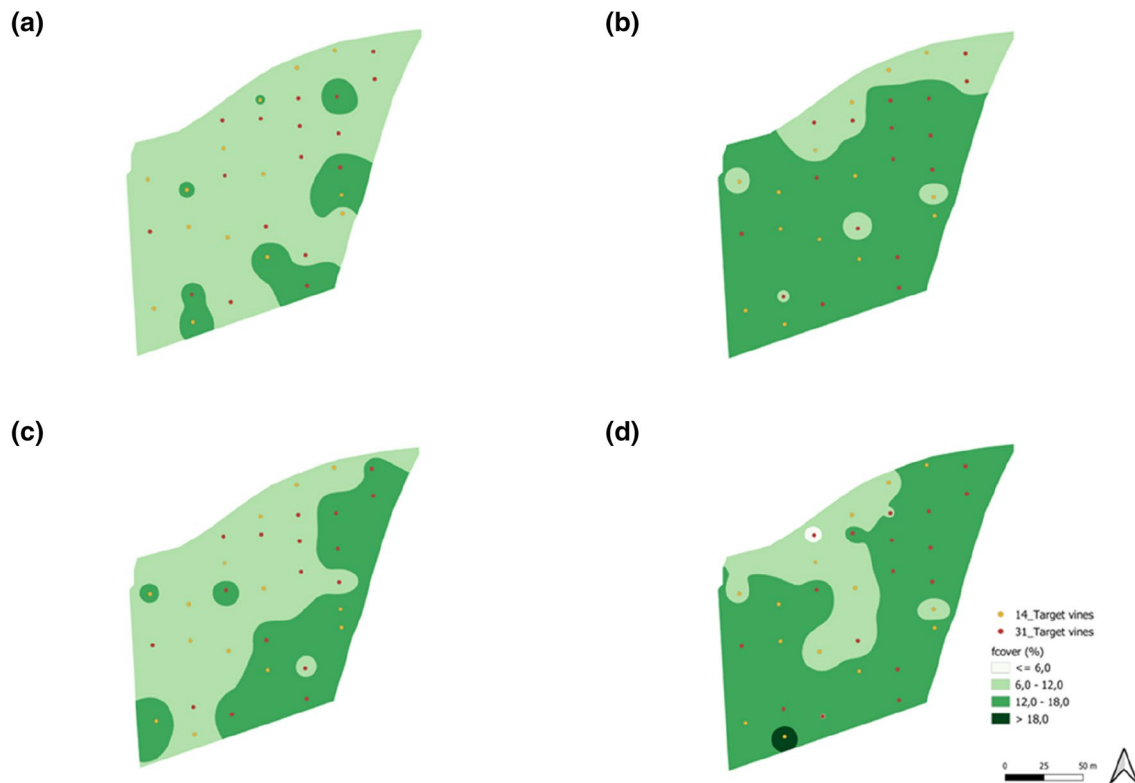12,0 - 18,0
> 18,0

0   25   50 m

Fig. 8 Spatial maps of f_{cover} (%) for the target vines for the four UAV flights at the different growth stages during the season. The colour scale represents the percentage of vegetation cover for the allocated polygon for each of the target vines on **a** DOY 363 **b** DOY 11 **c** DOY 25 **d** DOY 53

Variation recorded in temperature and relative humidity

In addition to f_{cover}, other environmental factors can influence plant water status and can serve as indicators of water stress. Here, we evaluated the relationship between Ψ_{SWP} and micrometeorological conditions by evaluating available weather station data compared to conditions in the canopy zone. Maximum temperature, corresponding RH and daily VPD was obtained from a nearby weather station (Fig. 10). Maximum temperature for the block ranged between 25 and 32 °C, RH between 34% and 40% and daily VPD ranged between 0.7 and 1.6 kPa.

In order to understand the effect of microclimate in the canopy zone on a spatial context, we evaluated the relationship between Ψ_{SWP} to maximum temperature, corresponding RH and VPD for each of the 14 target vines. Individual vines showed clear spatial variability with maximum temperatures in the canopy ranging from 33 to over 40 °C across the season (Fig. 11a–d). Corresponding RH ranged from 25 to above 40% (Fig. 11e–h). VPD measured in the individual canopies ranged from 3 to 8 kPa (Fig. 11i–l) with a CV 28.81%. The size and density of a vineyard's canopy have a profound impact on the microclimate (Smart 1985). A dense canopy with ample foliage provides significant shade, effectively reducing the intensity of direct sunlight exposure (Smart et al. 1988). This results in lower maximum temperatures within the canopy, as the shade prevents excessive heating during hot periods. Additionally, the canopy's density can trap moisture, leading to higher RH levels in the immediate vicinity. The influence of canopy size on VPD is also notable, as a larger and denser canopy helps maintain higher humidity levels by reducing water evaporation from the soil and transpiration from the leaves.

Potential water stress indicators

Following the analysis of VIs, NDVI exhibited the strongest correlation with Ψ_{SWP} with little difference between VI_{canopy} ($r = 0.57$) or VI_{mean} ($r = 0.53$) for grouped time points ($n = 124$). To explore the potential of using VIs along with f_{cover} and micrometeorological environmental parameters such as maximum temperature, RH, VPD and soil moisture as water stress indicators, a pairs plot (scatter matrix plot) analysis was performed with only relevant VIs reported (Fig. 12). This allows for the visualization

Fig. 9 Display the comparison between fractional cover (%) and stem water potential (Ψ_{SWP}) for three target vines, P2, P26 and P14. Each representing one of the stress water classes (Class 1 > −0.9 MPa, Class 2 between −0.9 and −1.2 MPa and Class 3 < −1.2 MPa). The developmental progress of fractional cover for each class from DOY 363 to DOY 53 is in grey, with corresponding Ψ_{SWP} values represented by a black line
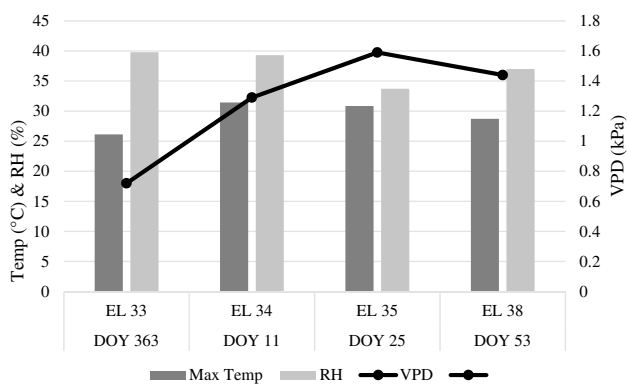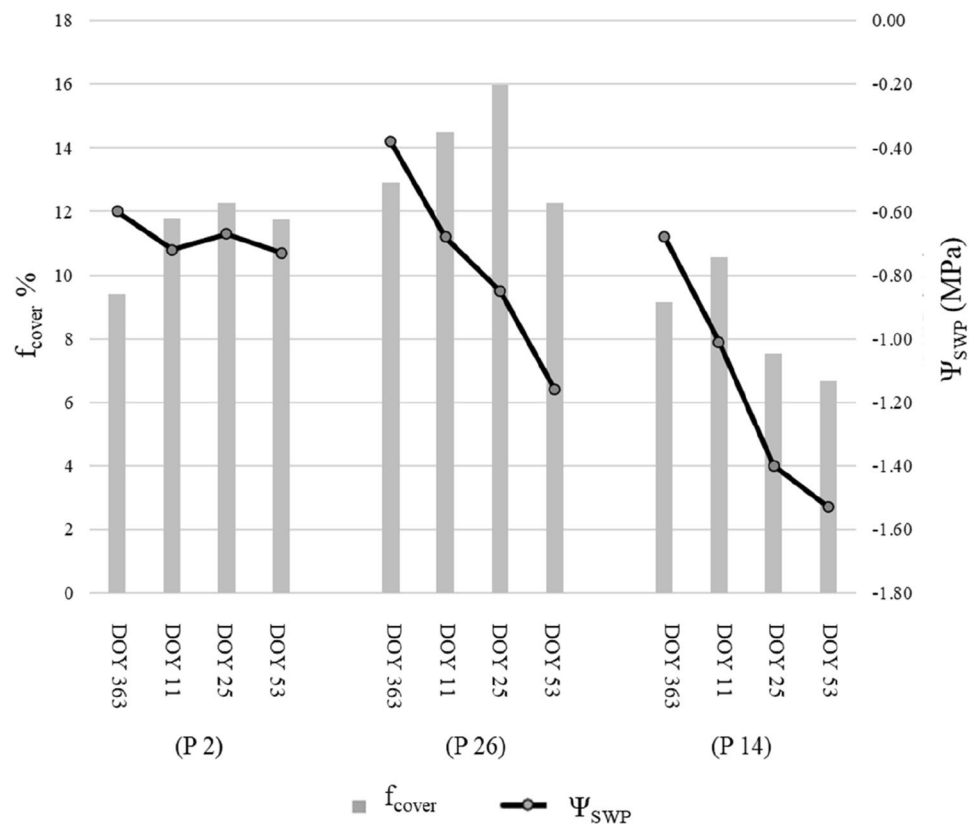

Fig. 10 Summary of the weather station data collected for the block corresponding to DOY 363 to DOY 53. The graph depicts the maximum temperature with corresponding RH measured for the specific date as well as the daily VPD measured

accuracy of future models for water stress monitoring and mapping. This analysis lays groundwork for work utilizing multilinear regression or machine learning models for predicting and mapping Ψ_{SWP} with bigger data sets.

The pairwise scatterplot results are presented in Fig. 12. A significant correlation ($p < 0.001$) was observed between Ψ_{SWP} and RH, $NDVI_{canopy}$, and $NDVI_{mean}$. Furthermore, there were notable correlations at the $p < 0.01$ level of significance between maximum temperature, VPD, and SWC_40 cm. Notably, both $NDVI_{canopy}$ and $NDVI_{mean}$ exhibited similar trends, displaying significant correlations with maximum temperature ($r = -0.341, -0.356$), RH ($r = 0.581, 0.475$), VPD ($r = -0.387, -0.361$), as well as SWC_20 cm ($r = -0.277$ and 0.341), respectively. These results highlight the intricate interplay between various environmental factors.

Discussion

Site-specific irrigation as defined by Cohen et al. (2005) is an irrigation practice that aims to provide irrigation at the smallest manageable scale matching in timing and amount to the actual crop need to achieve the desired crop response. Recent research by Pereyra et al. (2022) has demonstrated the potential benefits of site-specific irrigation on a small scale (intra-block), thanks to mapping carried out using
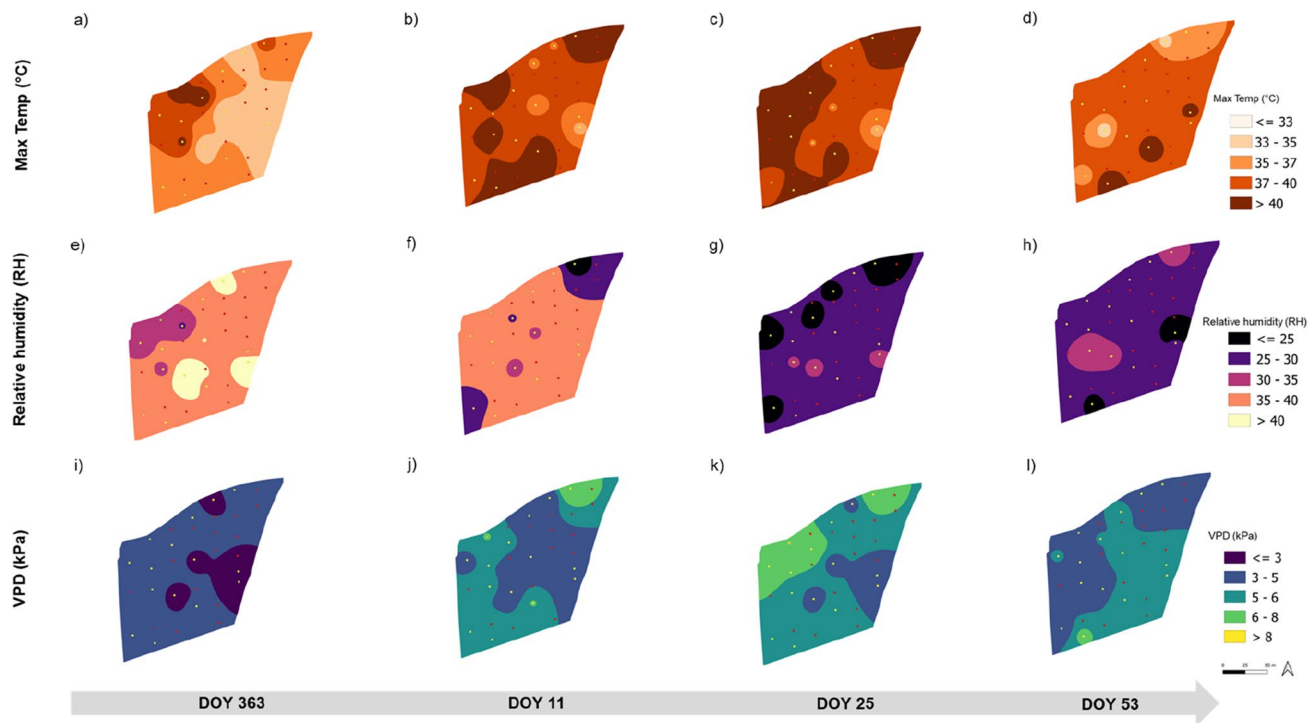
of multiple pairwise relationships between variables in a dataset. Each variable is plotted against all other variables. The diagonal plots show the distribution of each variable, while the upper and lower triangles show scatterplots of the pairwise combinations. Here we examined if the possible predictor variables had a linear association with the response variable which would indicate that a multiple linear regression model may be suitable. By identifying the parameters that show strong correlation with Ψ_{SWP}, we aim to improve

Fig. 11 Spatial variability shown by differences in maximum temperature (Max Temp), corresponding RH and VPD for individual target vines (*n* = 14) measured in the canopy zone. Spatial maps shown temporally for DOY 363 to DOY 53

precision viticulture technologies. To effectively implement precision irrigation strategies, monitoring parameters through spatial mapping can aid in decision-making. Traditional methods, such as stem water potential (Ψ_{SWP}), are not easily upscaled for monitoring intra-block variability, making non-destructive and fast methods necessary. Our study links to a recent study done by Borgogno-Mondino et al. (2022) aimed at testing the effectiveness of RS imagery in estimating and mapping Ψ_{SWP} in pomegranate plants. Their results showed promising capability of spectral indices of estimating Ψ_{SWP} readings. Interestingly their data showed that native data (mixed pixels) were found to be more effective in predicting Ψ_{SWP} than de-noised (un-mixed, pure pixels).

To explore the relationship between plant spectral indices obtained from high-resolution UAV multispectral data and midday stem water potential (Ψ_{SWP}), which is commonly used in irrigation decision-making, we designed a field experiment considering temporal and spatial intra-block variability. Additionally, we investigated the difference between pure (VI_{canopy}) and mixed (VI_{mean}) canopy pixels by utilizing canopy-based fraction segmentation. Water status variability in the block was confirmed for the 2020–2021 season, with maximum variability reached during véraison (DOY 25) with a coefficient of variance of 26.25%. At this stage, the range of Ψ_{SWP} was between −0.48 and −1.4 MPa, which included all three water stress classes

(Class 1 > −0.9 MPa; Class 2 between −0.9 and −1.2 MPa and Class 3 < −1.2 MPa), respectively, corresponding to literature levels of non-stress, moderately stressed and severely stressed vines (Van Leeuwen et al. 2009; Myburgh 2016). The evolution of SWC observed in our study was consistent with the findings of Davenport et al. (2008) which suggest that the spatial variability of soil water tends to decrease when water availability is higher, and water stress in the plant is lower. This phenomenon was particularly evident in the early stages of the growing season when SWC was relatively stable across the vineyard block, which could be attributed to the influence of winter precipitation (Fig. 4).

The relationship between Ψ_{SWP}, SWC, and f_{cover} that were observed in our data is consistent with the findings of previous studies that showed soil water availability influenced grapevine vegetative growth, cessation of shoot growth, reduction in leaf size, as well as high or early onset of leaf senescence (Kizildeniz et al. 2015; Wilson et al. 2020). Our study showed that most VIs displayed a negative correlation with Ψ_{SWP} indicating that the more stress the plant experienced due to water restrictions, VI values lowered. Less available water induces stress in the plants having lower fractional cover as they have less access to soil moisture, this can cause reduction in photosynthesis and growth, also reducing chlorophyll content.

Jones (2004) pointed out that greater precision in application of irrigation can potentially be obtained using
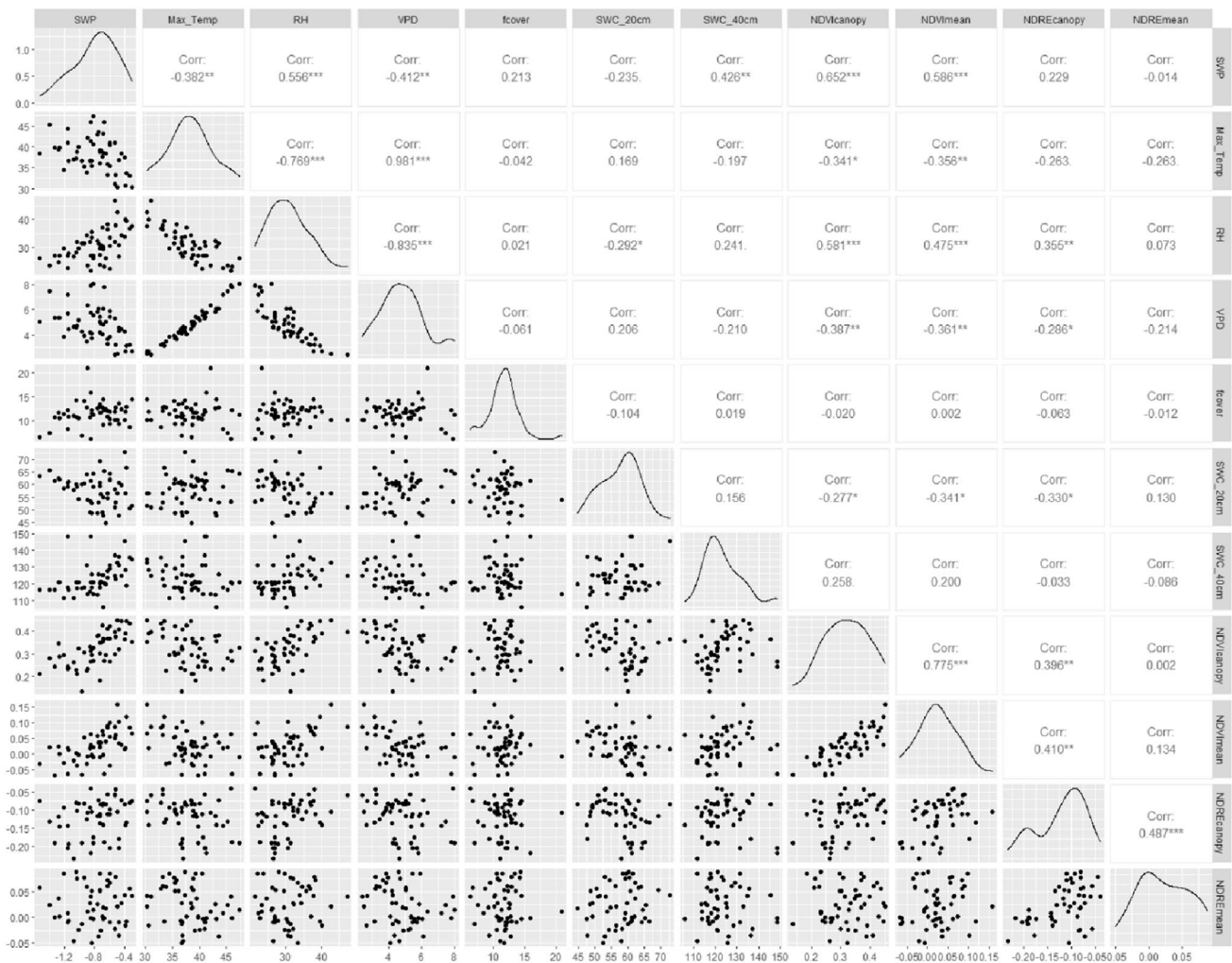
Fig. 12 Pairwise scatterplot matrix showing the correlation between variables of interest (Ψ_{SWP}, Temp, RH, f_{cover}, $NDVI_{canopy}$, $NDVI_{mean}$, $NDRE_{canopy}$ and $NDRE_{mean}$). Each scatterplot displays the relationship between two variables, with correlation coefficient (r) and p-values shown. *Asterisks () indicate the level of statistical significance for the Pearson correlation coefficient between two variables. The number of asterisks correspond to the level of significance, with one asterisk indicating $p < 0.05$, two asterisks indicating $p < 0.01$ and three asterisks indicating $p < 0.001$. For no asterisk, the correlation is not statistically significant at the 0.05 level

plant-based responses. In this sense, the use of reflectance indices can be a better indicator of water stress in comparison with measurements of soil water status (De Bei et al. 2011). Phenological stages such as, bud break, vegetative growth, flowering, fruit set, véraison, and harvest affect the vegetation characteristics. VIs assess changes in vegetation greenness, reflecting vigour and leaf area (Johnson et al. 2003; Zarco-Tejada et al. 2005; Ratana et al. 2006). These stages correspond to physiological processes in the grapevine growth cycle, resulting in changes in the plant. Soil water availability is crucial for plant development and phenology. Monitoring VIs over time, especially during critical phenological stages like véraison, can provide insight into soil conditions. VI_{mean} data suggest that that including the soil (mixed pixel) does indirectly account for changes in the canopy size during phenological stages (Fig. 7). Sustained decreases in VIs during specific stages may indicate water stress and lower Ψ_{SWP}. Prolonged water deficit can trigger acclimation responses, including growth inhibition as seen in f_{cover} of water stress class 3. The comparison between values from VI_{canopy} and VI_{mean} to Ψ_{SWP} relationship consistently showed a stronger relationship to VI_{mean} for individual dates. Although these VI values were very low (due to soil interferences), they did seem to show more potential in the monitoring of water stress than the pure canopy pixels as in accordance with (Borgogno-Mondino et al. 2022). Regarding canopy characterization from VI, it is important to note the VI is primarily sensitive to the density as it is only representative of the top of the canopy rather than its size or shape. This suggest that the water status of two

canopies with the same VI_{canopy} could vary depending on their shape or size. Pure pixels VIs provide a valuable means of accurately assessing canopy density, chlorophyll content and overall plant health due to their focus on vegetation-specific characteristics and generally tend to have higher VI values (Hall et al. 2002, 2003) However, they do not directly account for the size or vigour of the vegetation, as these factors can be influenced by soil properties and other variables. Incorporating mixed pixel approaches that consider both vegetation and soil components can indirectly account for size and provide a more comprehensive understanding of plant growth dynamics. However, mixed pixels including cover crop and not bare soil, can lead to biased values (Khaliq et al. 2019). Alternatively, combining pure pixel VIs with measures such as f_{cover}, which integrates information about vegetation size, we can achieve better correlation with soil water potential and obtain a more comprehensive evaluation of vegetation vigour and its relationship to soil moisture conditions. When the dataset was combined for the season, no significant differences in correlation was found for $NDVI_{mean}$ and $NDVI_{canopy}$ ($r = 0.53$ vs $r = 0.57$), having the strongest correlation of all the VIs. Stronger correlations were also found by Hall et al. (2008) when phenological stages were combined instead of evaluating correlations of individual phenological stages. A few small-scale UAV studies with multispectral imagery have also found that various VIs are significantly correlated with grapevine water stress levels (Baluja et al. 2012; Espinoza et al. 2017).

The use of VIs raises several questions regarding application. VIs appears to show better correlations when correlating with biophysical parameters such as biomass yield when pure extraction methods such as photogrammetry or pixel classification algorithms (e.g., ANN, RF, thresholding, or DEM-models), are employed. These approaches exhibit significant success in distinguishing between groups and rows, particularly in studies focusing on bare soil, compared to more challenging scenarios involving cover crops and shaded pixels, but their effectiveness in assessing water stress still seems limited. Most studies only obtained moderate correlations, and only when seasonal data are grouped. To improve correlations, integrated methods incorporating additional parameters are suggested. Canopy temperature is a well-known indicator of plant water status and has been considered as a potential tool for irrigation scheduling (Costa et al. 2010; Jones 1999). Other factors, such as solar radiation, water availability, and RH, also strongly influence grapevine growth and development. In our study, we found that the highest temperatures were experienced during January (E-L34 and E-L35) with increasing VPD levels as the temperature increased. This corresponds to increasing Ψ_{SWP} trends towards harvest, providing context for spatial patterns in relation to water stress. To evaluate the potential of additional parameters as water stress indicators

for future mapping, we monitored 14 target vines. These results showed that the integration of NDVI with additional information on maximum temperature, RH and f_{cover} could be used to map water stress variability. The findings also revealed interesting correlation between $NDVI_{mean}$ and SWC_20 cm, surpassing those observed by $NDVI_{canopy}$. These results suggest that mixed pixels not only reflect variation in canopy size but also indirectly capture soil properties, such as soil moisture (Hall et al. 2003; Towers and Poblete-Echeverría 2021). This indirect relationship may be attributed to the potential influence of larger canopies and shading perhaps reducing soil evapotranspiration. Thus, the inclusion of $NDVI_{mean}$ offers a promising avenue to indirectly incorporate both canopy characteristics and soil properties for simplified mapping of water stress. The findings is consistent with Acevedo-Opazo et al. (2008) who suggested to include three sections when evaluating water stress variability: (1) description of plant water status based on direct measurements on plants (ground truthing); (2) plant water status assessment based on auxiliary information (i.e. weather, soil, and plant vegetative expression); and (3) a proposal for combining local reference measurements and auxiliary information to characterise the spatial variability of the vine water status in the vineyard scale.

Conclusion

This study evaluated if fraction-based segmentation, to obtain pure canopy VIs of individual target vines, could be used to map water status variability using pure VIs within a commercial vineyard block. This was done by correlating field data measurements of midday Ψ_{SWP} and SWC with pure (VI_{canopy}) and mixed pixel (VI_{mean}) data. When analysing pure canopy pixels, the VI values may provide more accurate representation of canopy density and chlorophyll content as well as overall health, although size may indirectly be accounted for in mixed pixel data. The use of VIs in context of assessing water stress raises several important considerations. Although pure extraction methods are successful in classifying pixels distinguishing between different groups (inter-row, canopy, soil) it has been observed that VIs tend to exhibit stronger correlations with mixed pixels in the application of evaluating water stress. The analysis of environmental parameters, such as maximum temperature, RH and VPD, in relation to Ψ_{SWP} provide further insights into the microclimate's influence on plant water status. The pairwise scatterplot analysis revealed significant correlations between Ψ_{SWP}, maximum temperature, RH, VPD, SWC_40 cm, $NDVI_{canopy}$ and $NDVI_{mean}$. The findings suggest that multispectral data, along with environmental parameters, have the potential to be utilized for precision irrigation management and monitoring water stress at a finer spatial scale.

However, it was acknowledged that the limitations of VI measurements, such as the masking of important variations in vegetation characteristics, need to be addressed either by using mixed pixels or considering the use of f_{cover}. Overall, our study adds to the existing literature by demonstrating the potential of high-resolution UAV multispectral data and VI to monitor intra-block variability in water stress as a guide for precision irrigation management practices. The high spatial resolution offered by UAV sensors, often reaching the centimetre level, is a remarkable advantage. This capability not only allows for the segmentation of pure pixels but also greatly enhances the differentiation of various objects within the image, including details within canopies (Khaliq et al. 2019). This emphasis on spatial resolution highlights its significance in RS applications for precision agriculture and environmental monitoring. Future research should focus on assessing the influence of diverse vineyard microclimate on the interplay between environmental parameters, VIs, and water stress. Additionally, exploring data fusion techniques for the integration of data from multiple sources, such as RS, weather stations, and soil moisture sensors, offers the potential to enhance the accuracy of water stress assessments, thereby optimizing decision-making processes in vineyard management. In conclusion, the research conducted in this study, in line with findings of Van Leeuwen et al. (2019), highlights the potential of utilizing vineyard attributes in their interrelations with irrigation regimes for implementing smart irrigation practices.

Declarations

References

Acevedo-Opazo C, Tisseyre B, Ojeda H, Ortega-Farias S, Guillaume S (2008) Is it possible to assess the spatial variability of vine water status? J Int Des Sci La Vigne Du Vin 42:203–220. https://doi.org/10.20870/oeno-one.2008.42.4.811

Ahmad U, Alvino A, Marino S (2021) A review of crop water stress assessment using remote sensing. Remote Sens 13(20):4155. https://doi.org/10.3390/rs13204155

Baluja J, Diago MP, Balda P, Zorer R, Meggio F, Morales F, Tardaguila J (2012) Assessment of vineyard water status variability by thermal and multispectral imagery using an unmanned aerial vehicle (UAV). Irrig Sci 30:511–522. https://doi.org/10.1007/s00271-012-0382-9

Barnes EM, Clarke TR, Richards SE, Colaizzi PD, Haberland J, Kostrzewhki M, Waller P, Choi CRE, Thompson T, Lascano RJ, Li H, Moran MS (2000) Coincident detection of crop water stress, nitrogen status and canopy density using ground based multispectral data. In: Proc 5th Int Conf Precis Agric July

Borgogno-Mondino E, Farbo A, Novello V, de Palma L (2022) A fast regression-based approach to map water status of pomegranate orchards with sentinel 2 data. Horticulturae 8:1–16. https://doi.org/10.3390/horticulturae8090759

Burgos S, Mota M, Noll D, Cannelle B (2015) Use of Very high-resolution airborne images to analyse 3D canopy architecture of a vineyard. ISPRS Int Arch Photogramm Remote Sens Spat Inf Sci 33:399–403. https://doi.org/10.5194/isprsarchives-xl-3-w3-399-2015

Calvario G, Sierra B, Alarcón TE, Hernandez C, Dalmau O (2017) A multi-disciplinary approach to remote sensing through low-cost UAVs. Sensors 17:1411. https://doi.org/10.3390/s17061411

Caruso G, Tozzini L, Rallo G, Primicerio J, Moriondo M, Palai G, Gucci R (2017) Estimating biophysical and geometrical parameters of grapevine canopies ('Sangiovese') by an unmanned aerial vehicle (UAV) and VIS-NIR cameras. Vitis 56:63–70. https://doi.org/10.5073/vitis.2017.56.63-70

Chaves MM, Santos TP, Souza CD, Ortuño M, Rodrigues M, Lopes C, Maroco J, Pereira JS (2007) Deficit irrigation in grapevine improves water-use efficiency while controlling vigour and production quality. Ann Appl Biol 150:237–252. https://doi.org/10.1111/j.1744-7348.2006.00123.x

Chaves MM, Zarrouk O, Francisco R, Costa JM, Santos T, Regalado AP, Rodrigues ML, Lopes CM (2010) Grapevine under deficit irrigation: hints from physiological and molecular data. Ann Bot 105:661–676. https://doi.org/10.1093/aob/mcq030

Choné X, Van Leeuwen C, Dubourdieu D, Gaudillère JP (2001) Stem water potential is a sensitive indicator of grapevine water status. Ann Bot 87:477–483. https://doi.org/10.1006/anbo.2000.1361

Cinat P, Di Gennaro SF, Berton A, Matese A (2019) Comparison of unsupervised algorithms for vineyard canopy segmentation from UAV multispectral images. Remote Sens 11:1–24. https://doi.org/10.3390/rs11091023

Cogato A, Jewan SYY, Wu L, Marinello F, Meggio F, Sivilotti P, Sozzi M, Pagay V (2022) Water stress impacts on grapevines (*Vitis vinifera* L.) in hot environments: physiological and spectral responses. Agronomy 12(8):1819. https://doi.org/10.3390/agronomy12081819

Cohen Y, Alchanatis V, Meron M, Saranga S, Tsipris J (2005) Estimation of leaf water potential by thermal imagery and spatial analysis. J Exp Bot 56:1843–1852. https://doi.org/10.1093/jxb/eri174

Costa JM, Grant OM, Chaves MM (2010) Use of thermal imaging in viticulture: current application and future prospects. In: Delrot S, Medrano H, Or E, Bavaresco L, Grando S (eds) Methodologies and results in grapevine research. Springer, New York, pp 135–150

Davenport JR, Stevens RG, Whitley KM (2008) Spatial and temporal distribution of soil moisture in drip-irrigated vineyards. HortScience 43:229–235. https://doi.org/10.21273/hortsci.43.1.229

De Bei R, Cozzolino D, Sullivan W, Cynkar W, Fuentes S, Dambergs R, Pech J, Tyerman S (2011) Non-destructive measurement of grapevine water potential using near infrared spectroscopy. Aust J Grape Wine Res 17:62–71. https://doi.org/10.1111/j.1755-0238.2010.00117.x

de Castro AI, Torres-Sánchez J, Peña JM, Jiménez-Brenes FM, Csillik O, López-Granados F (2018) An automatic random forest-OBIA algorithm for early weed mapping between and within crop rows using UAV imagery. Remote Sens 10:285. https://doi.org/10.3390/rs10020285

Coombe BG (1995) Growth Stages of the Grapevine: Adoption of a system for identifying grapevine growth stages. Aust J Grape Wine Res 1(2):104–110. https://doi.org/10.1111/j.1755-0238.1995.tb00086.x

Eichhorn KW, Lorenz DH (1977) Phenological development stages of the grape vine. Nachrichtenblatt desdeutschen Pflanzenschutzdienstes 29(8):119–120

Di Gennaro SF, Rizza F, Badeck FW, Berton A, Delbono S, Gioli B, Toscano P, Zaldei A, Matese A (2018) UAV-based high-throughput phenotyping to discriminate barley vigour with visible and near-infrared vegetation indices. Int J Remote Sens 39:5330–5344. https://doi.org/10.1080/01431161.2017.1395974

Di Gennaro SF, Dainelli R, Palliotti A, Toscano P, Matese A (2019) Sentinel-2 validation for spatial variability assessment in overhead trellis system viticulture versus UAV and agronomic data. Remote Sens 11(21):2573. https://doi.org/10.3390/rs11212573

Dobrowski SZ, Ustin SL, Wolpert JA (2002) Remote estimation of vine canopy density in vertically shoot-positioned vineyards: determining optimal vegetation indices. Aust J Grape Wine Res 8:117–125. https://doi.org/10.1111/j.1755-0238.2002.tb00220.x

Espinoza CZ, Khot LR, Sankaran S, Jacoby PW (2017) High resolution multispectral and thermal remote sensing-based water stress assessment in subsurface irrigated grapevines. Remote Sens 9(9):961. https://doi.org/10.3390/rs9090961

Ezenne GI, Jupp L, Mantel SK, Tanner JL (2019) Current and potential capabilities of UAS for crop water productivity in precision agriculture. Agric Water Manag 218:158–164

Filippetti I, Allegro G, Valentini G, Pastore C, Colucci E, Intrieri C (2013) Influence of vigour on vine performance and berry composition of cv. Sangiovese (Vitis vinifera L.). J Int Des Sci La Vigne Du Vin 47:21–33. https://doi.org/10.20870/oeno-one.2013.47.1.1534

Gago J, Douthe C, Coopman RE, Gallego PP, Ribas-Carbo M, Flexas J, Escalona J, Medrano H (2015) UAVs challenge to assess water stress for sustainable agriculture. Agric Water Manag 153:9–19. https://doi.org/10.1016/j.agwat.2015.01.020

Gatti M, Garavani A, Vercesi A, Poni S (2017) Ground-truthing of remotely sensed within-field variability in a cv. Barbera plot for improving vineyard management. Aust J Grape Wine Res 23(3):399–408. https://doi.org/10.1111/ajgw.12286

Gautam D, Pagay V (2020) A review of current and potential applications of remote sensing to study the water status of horticultural crops. Agronomy 10(1):140. https://doi.org/10.3390/agronomy10010140

Gilbert N (2012) Water under pressure. Nature 483:256–257. https://doi.org/10.1038/483256a

Giovos R, Tassopoulos D, Kalivas D, Lougkos N, Priovolou A (2021) Remote sensing vegetation indices in viticulture: a critical review. Agriculture (switzerland) 11(5):457. https://doi.org/10.3390/agriculture11050457

Gitelson AA, Merzlyak MN (1997) Remote estimation of chlorophyll content in higher plant leaves. Int J Remote Sens 18:2691–2697. https://doi.org/10.1080/014311697217558

Hall A, Lamb DW, Holzapfel B, Louis J (2002) Optical remote sensing applications in viticulture—a review. Aust J Grape Wine Res 8:36–47. https://doi.org/10.1111/j.1755-0238.2002.tb00209.x

Hall A, Louis JP, Lamb DW (2003) A method for vineyard attribute mapping from high resolution multispectral images. Comput Geosci 29:813–822. https://doi.org/10.1016/s0098-3004(03)00082-7

Hall A, Louis JP, Lamb DW (2008) Low resolution remotely sensed images of winegrape vineyards map spatial variability in planimetric canopy area instead of leaf area index. Aust J Grape Wine Res 14:9–17. https://doi.org/10.1111/j.1755-0238.2008.00002.x

Hassan-Esfahani L, Torres-Rua A, Jensen A, McKee M (2015) Assessment of surface soil moisture using high-resolution multi-spectral imagery and artificial neural networks. Remote Sens 7:2627–2646. https://doi.org/10.3390/rs70302627

Huang DY, Lin TW, Hu WC (2011) Automatic multilevel thresholding based on two-stage Otsu's method with cluster determination by valley estimation. Int J Innov Comput Inf Control 7:5631–5644. https://doi.org/10.21203/rs.3.rs-2750189/v1

Huete AR (1988) A soil-adjusted vegetation index (SAVI). Remote Sens Environ 25:295–309. https://doi.org/10.1016/0034-4257(88)90106-x

Jasse A, Berry A, Aleixandre-Tudo JL, Poblete-Echeverría C (2021) Intra-block spatial and temporal variability of plant water status and its effect on grape and wine parameters. Agric Water Manag 246:106696. https://doi.org/10.1016/j.agwat.2020.106696

Johnson LF, Roczen DE, Youkhana SK, Nemani RR, Bosch DF (2003) Mapping vineyard leaf area with multispectral satellite imagery. Comput Electron Agric 38:33–44. https://doi.org/10.1016/S0168-1699(02)00106-0

Jones HG (1999) Use of infrared thermometry for estimation of stomatal conductance as a possible aid to irrigation scheduling. Agric for Meteorol 95:139–149. https://doi.org/10.1016/s0168-1923(99)00030-1

Jones HG (2004) Application of thermal imaging and infrared sensing in plant physiology and ecophysiology. Adv Bot Res 41:107–163. https://doi.org/10.1016/s0065-2296(04)41003-9

Karpina M, Jarzabek-Rychard M, Tymków P, Borkowski A (2016) UAV-based automatic tree growth measurement for biomass estimation. Int Arch Photogram Remote Sens Spatial Inform Sci ISPRS Arch 41:685–688. https://doi.org/10.5194/isprsarchives-XLI-B8-685-2016

Kerkech M, Hafiane A, Canals R (2020) Vine disease detection in UAV multispectral images using optimized image registration and deep learning segmentation approach. Comput Electron Agric 174:105446. https://doi.org/10.1016/j.compag.2020.105446

Khaliq A, Comba L, Biglia A, Ricauda Aimonino D, Chiaberge M, Gay P (2019) Comparison of satellite and UAV-based multispectral imagery for vineyard variability assessment. Remote Sens 11(4):436. https://doi.org/10.3390/rs11040436

Kizildeniz T, Mekni I, Santesteban H, Pascual I, Morales F, Irigoyen JJ (2015) Effects of climate change including elevated CO_2 concentration, temperature and water deficit on growth, water status, and yield quality of grapevine (Vitis vinifera L.) cultivars. Agric Water Manag 159:155–164. https://doi.org/10.1016/j.agwat.2015.06.015

Liu Y, Mu X, Wang H, Yan G (2012) A novel method for extracting green fractional vegetation cover from digital images. J Veg Sci 23:406–418. https://doi.org/10.1111/j.1654-1103.2011.01373.x

Maimaitiyiming M, Sagan V, Sidike P, Maimaitijiang M, Miller AJ, Kwasniewski M (2020) Leveraging very-high spatial resolution hyperspectral and thermal UAV imageries for characterizing diurnal indicators of grapevine physiology. Remote Sens 12:1–30. https://doi.org/10.3390/rs12193216

Matese A, Di Gennaro SF (2015) Technology in precision viticulture: a state of the art review. Int J Wine Res 7(1):69–81. https://doi.org/10.2147/IJWR.S69405

Matese A, Toscano P, Di Gennaro SF, Genesio L, Vaccari FP, Primicerio J, Belli C, Zaldei A, Bianconi R, Gioli B (2015) Intercomparison of UAV, aircraft and satellite remote sensing platforms for precision viticulture. Remote Sens 7(3):2971–2990. https://doi.org/10.3390/rs70302971

Matese A, Baraldi R, Berton A, Cesaraccio C, Di Gennaro SF, Duce P, Facini O, Mameli MG, Piga A, Zaldei A (2018) Estimation of water stress in grapevines using proximal and remote sensing methods. Remote Sens 10(1):114. https://doi.org/10.3390/rs10010114

Matese A, Di Gennaro SF, Santesteban LG (2019) Methods to compare the spatial variability of UAV-based spectral and geometric information with ground autocorrelated data. A case of study for precision viticulture. Comput Electron Agric 162:931–940. https://doi.org/10.1016/j.compag.2019.05.038

Motohka T, Nasahara KN, Oguma H, Tsuchida S (2010) Applicability of green-red vegetation index for remote sensing of vegetation phenology. Remote Sens 2:2369–2387. https://doi.org/10.3390/rs2102369

Myburgh PA (2016) Estimating transpiration of whole grapevines under field conditions. S Afr J Enol Vitic 37:47–60. https://doi.org/10.21548/37-1-758

Pádua L, Marques P, Hruška J, Adão T, Bessa J, Sousa A, Peres E, Morais R, Sousa JJ (2018) Vineyard properties extraction combining UAS-based RGB imagery with elevation data. Int J Remote Sens 39:5377–5401. https://doi.org/10.1080/01431161.2018.1471548

Pádua L, Adão T, Sousa A, Peres E, Sousa JJ (2020) Individual grapevine analysis in a multi-temporal context using UAV-based multi-sensor imagery. Remote Sens 12:139. https://doi.org/10.3390/rs12010139

Pádua L, Matese A, Di Gennaro SF, Morais R, Peres E, Sousa JJ (2022) Vineyard classification using OBIA on UAV-based RGB and multispectral data: a case study in different wine regions. Comput Electron Agric 196:106905. https://doi.org/10.1016/j.compag.2022.106905

Pagay V, Kidman CM (2019) Evaluating remotely-sensed grapevine (*Vitis vinifera* L.) water stress responses across a viticultural region. Agronomy 9(11):682. https://doi.org/10.3390/agronomy9110682

Pereyra G, Pellegrino A, Gaudin R, Ferrer M (2022) Evaluation of site-specific management to optimise *Vitis vinifera* L. (cv. Tannat) production in a vineyard with high heterogeneity. Oeno One 56:397–412. https://doi.org/10.20870/oeno-one.2022.56.3.5485

Poblete-Echeverría C, Tardaguila J (2023) Digital technologies: smart applications in viticulture. In: Encyclopedia of smart agriculture technologies, pp 1–13. https://doi.org/10.1007/978-3-030-89123-7_206-1

Ratana P, Huete AR, Didan K (2006) MODIS EVI-based variability in Amazon phenology across the rainforest-cerrado ecotone. In: 2006 geoscience and remote sensing symposium 1–8, pp 1942–1944. https://doi.org/10.1109/Igarss.2006.502

Rodríguez-Pérez JR, Ordóñez C, González-Fernández AB, Sanz-Ablanedo E, Valenciano JB, Marcelo V (2018) Leaf water content estimation by functional linear regression of field spectroscopy data. Biosyst Eng 165:36–46. https://doi.org/10.1016/j.biosystemseng.2017.08.017

Romboli Y, Di Gennaro SF, Mangani S, Buscioni G, Matese A, Genesio L, Vincenzini M (2017) Vine vigour modulates bunch microclimate and affects the composition of grape and wine flavonoids: an unmanned aerial vehicle approach in a Sangiovese vineyard in Tuscany. Aust J Grape Wine Res 23:368–377. https://doi.org/10.1111/ajgw.12293

Rossini M, Fava F, Cogliati S, Meroni M, Marchesi A, Panigada C, Giardino C, Busetto L, Migliavacca M, Amaducci S et al (2013) Assessing canopy PRI from airborne imagery to map water stress in maize. ISPRS J Photogramm Remote Sens 86:168–177. https://doi.org/10.1016/j.isprsjprs.2013.10.002

Rouse J, Haas RH, Schell JA, Deering DW, Harlan JC (1974) Monitoring the vernal advancement and retrogradation (Green-wave effect) of natural vegetation. RS Center, A Texas, GSF Center—1974—Texas A &M University, Remote Sensing Center

Santesteban LG, Di Gennaro SF, Herrero-Langreo A, Miranda C, Royo JB, Matese A (2017) High-resolution UAV-based thermal imaging to estimate the instantaneous and seasonal variability of plant water status within a vineyard. Agric Water Manag 183:49–59. https://doi.org/10.1016/j.agwat.2016.08.026

Saxton KE, Rawls WJ (2006) Soil water characteristic estimates by texture and organic matter for hydrologicsolutions. Soil Sci Soc Am J 70(5):1569–1578. https://doi.org/10.1016/10.2136/sssaj2005.0117

Smart RE (1985) Principles of grapevine canopy microclimate manipulation with implications for yield and quality. J Ecol 36(3):230–239

Smart RE, Smith SM, Winchester RV (1988) Light quality and quantity effects on fruit ripening for Cabernet Sauvignon. Am J Enol Vitic 39(3):250–258. https://doi.org/10.5344/ajev.1988.39.3.250

Sozzi M, Kayad A, Marinello F, Taylor JA, Tisseyre B (2020) Comparing vineyard imagery acquired from sentinel-2 and unmanned aerial vehicle (UAV) platform. Oeno One 54:189–197. https://doi.org/10.20870/oeno-one.2020.54.2.2557

Stocker TF, Qin D, Plattner GK, Tignor M, Allen SK, Boschung J, Nauels A, Xia Y, Bex V, Midgley PM (2013) IPCC climate change: the physical science basis. Contribution of Working Group I to the Fifth Assessment Report of the Intergovernmental Panel on Climate Change. Cambridge University Press, Cambridge, UK/New York, NY, USA

Suárez L, Zarco-Tejada PJ, Sepulcre-Cantó G, Pérez-Priego O, Miller JR, Jiménez-Muñoz J, Sobrino J (2008) Assessing canopy PRI for water stress detection with diurnal airborne imagery. Remote Sens Environ 112:560–575. https://doi.org/10.1016/j.rse.2007.05.009

Tang Z, Jin Y, Alsina MM, McElrone AJ, Bambach N, Kustas WP (2022) Vine water status mapping with multispectral UAV imagery and machine learning. Irrig Sci 40:715–730. https://doi.org/10.1007/s00271-022-00788-w

Tardaguila J, Stoll M, Gutiérrez S, Proffitt T, Diago MP (2021) Smart applications and digital technologies in viticulture: a review. Smart Agric Technol 1:100005. https://doi.org/10.1016/j.atech.2021.100005

Thorp K, Thompson A, Harders S, French A, Ward R (2018) High-throughput phenotyping of crop water use efficiency via multispectral drone imagery and a daily soil water balance model. Remote Sens 10:1682. https://doi.org/10.3390/rs10111682

Tiozzo Fasiolo D, Pichierri A, Sivilotti P, Scalera L (2023) An analysis of the effects of water regime on grapevine canopy status using a UAV and a mobile robot. Smart Agric Technol 6:100344. https://doi.org/10.1016/j.atech.2023.100344

Towers P, Poblete-Echeverría C (2021) Effect of the illumination angle on NDVI data composed of mixed surface values obtained over vertical-shoot-positioned vineyards. Remote Sens 13(5):855. https://doi.org/10.3390/rs13050855

van Leeuwen C, Trégoat O, Choné X, Bois B, Pernet D, Gaudillère JP (2009) Vine water status is a key factor in grape ripening and vintage quality for red Bordeaux wine. How can it be assessed for vineyard management purposes? J Int Sci Vigne Vin 43:121–134. https://doi.org/10.20870/oeno-one.2009.43.3.798

Van Leeuwen C, Roby JP, De Rességuier L (2018) Soil-related terroir factors: a review. Oeno One 52:173–188. https://doi.org/10.20870/oeno-one.2018.52.2.2208

Van Leeuwen C, Pieri P, Gowdy M, Olla N, Roby C (2019) Reduced density is an environmental friendly and cost effective solution to increase resilience to drought in vineyards in a context of climate change. Oeno One 53:129–146. https://doi.org/10.20870/oeno-one.2019.53.2.2420

Wilson TG, Kustas WP, Alfieri JG, Anderson MC, Gao F, Prueger JH, McKee LG, Alsina MM, Sanchez LA, Alstad KP (2020) Relationships between soil water content, evapotranspiration, and irrigation measurements in a California drip irrigated Pinot noir vineyard. Agric Water Manag 237:106186. https://doi.org/10.1016/j.agwat.2020.106186

Zarco-Tejada PJ, Berjón A, López-Lozano R, Miller JR, Martín P, Cachorro V, Gonzales MR, de Frutos A (2005) Assessing vineyard condition with hyperspectral indices: leaf and canopy reflectance simulation in a row-structured discontinuous canopy. Remote Sens Environ 99:271–287. https://doi.org/10.1016/j.rse.2005.09.002

Zarco-Tejada PJ, Suárez L, González-Dugo V (2013) Spatial resolution effects on chlorophyll fluorescence retrieval in a heterogeneous canopy using hyperspectral imagery and radiative transfer simulation. IEEE Geosci Remote Sens 10:937–941. https://doi.org/10.1109/lgrs.2013.2252877

Zúñiga M, Ortega-Farías S, Fuentes S, Riveros-Burgos C, Poblete-Echeverría C (2018) Effects of three irrigation strategies on gas exchange relationships, plant water status, yield components and water productivity on grafted Carmenere grapevines. Front Plant Sci 9:992. https://doi.org/10.3389/fpls.2018.00992

Publisher's Note Springer Nature remains neutral with regard to jurisdictional claims in published maps and institutional affiliations.